Electric current density imaging via an accelerated iterative algorithm with joint sparsity constraints

Gabriella Bretti, Massimo Fornasier, Francesca Pitolli

Electric current density imaging via an accelerated iterative algorithm with joint sparsity constraints

Gabriella Bretti
Me.Mo.Mat Department of the University "La Sapienza" of Rome, Via A. Scarpa, 00161 Rome, Italy
Email: gab.bretti@gmail.com

Massimo Fornasier
Johann Radon Institute for Computational and Applied Mathematics of Linz Altenbergerstrasse 69 A-4040 Linz, Austria
Email: massimo.fornasier@oeaw.ac.at

Francesca Pitolli
Me.Mo.Mat Department of the University "La Sapienza" of Rome, Via A. Scarpa, 00161 Rome, Italy
Email: pitolli@dmmm.uniroma1.it

***Abstract*—Many problems in applied sciences require to spatially resolve an unknown electrical current distribution from its external magnetic field. Electric currents emit magnetic fields which can be measured by sophisticated superconducting devices in a noninvasive way. Applications of this technique arise in several fields, such as medical imaging and non-destructive testing, and they involve the solution of an inverse problem.**

Assuming that each component of the current density vector possesses the same sparse representation with respect to a preassigned multiscale basis, allows us to apply new regularization techniques to the magnetic inverse problem.

The solution of linear inverse problems with sparsity constraints can be efficiently obtained by iterative algorithms based on gradient steps intertwined with thresholding operations. We test this algorithms to numerically solve the magnetic inverse problem with a joint sparsity constraint.

I. Introduction

Many problems in applied sciences require to map the spatial distribution of electric currents flowing through a given sample. For example, in neuroscience studies the brain activity can be localized by detecting the regions where neural currents flow. Similarly, in nondestructive testing cracks and corrosion damage in a structure result in perturbations of the current flow.

A given electric current distribution produces a characteristic magnetic field which provides information on the process occurring within the object. Since the magnetic field decreases fast as the distance from the current source to the sensor position increases, the magnetic data can be affected by a high noise. Usually, the measurements are obtained by SQUID magnetometers, that can detect magnetic fields generated by deep currents in a noninvasive way [14].

Of course the magnetic data do not give an immediate image of the current distribution, hence we have to solve the associated inverse problem and regularization techniques are needed [1],[13]. The Tikhonov regularization with quadratic constraint, gives good results when the quantities under observation are equally distributed in time or space [7]. However, in the applications we are interested in, the regions where the currents flow are usually small, hence the current distribution is spatially inhomogeneous, and can be represented as a sum of weighted basic currents with only few relevant terms.

To promote a sparse representation regularization techniques based on ℓ_1-minimization have been introduced, see, e.g., [6]. In the case the quantity of interest can be modelled as a vector-valued signal with jointly sparse components, then the regularizations introduced in [9], [10] are more suited, see also [2], [8], [12].

Iterative thresholding algorithms have been proposed for the solution of inverse problems with sparsity constraints, but they have shown rather slow performances in the magnetic

tomography problem. In this paper we would like to proposed also for the joint-sparsity constraints a modification inspired by [5] where the thresholding operations are substituted with suitable projections onto convex sets. These projections turn out to be simply adaptive thresholding steps. For classical sparsity constraints based on ℓ_1-minimization this approach has shown significant speed improvements in practice.

II. The Forward and Inverse Magnetic Problems

From the quasi-static Maxwell's equations it follows that the magnetic field $\vec{\mathbf{B}}$ generated by a current density $\vec{\mathbf{J}}$ obeys the *Biot-Savart law*:

$$\vec{\mathbf{B}}(\vec{\mathbf{J}},\vec{\mathbf{r}}) = \frac{\mu_0}{4\pi}\int_{V_0} \vec{\mathbf{J}}(\vec{\mathbf{r}}\,') \times \frac{(\vec{\mathbf{r}}-\vec{\mathbf{r}}\,')}{|\vec{\mathbf{r}}-\vec{\mathbf{r}}\,'|^3}\, d\vec{\mathbf{r}}\,', \qquad (2.1)$$

where μ_0 is the magnetic permeability in the vacuum and V_0 is the region where the current flows. Usually, the magnetometers measure just the normal component of the magnetic field, whose expression is given by

$$B_e(\vec{\mathbf{J}},\vec{\mathbf{r}}) = \frac{\mu_0}{4\pi}\int_{V_0} \frac{\vec{\mathbf{e}}(\vec{\mathbf{r}})\times(\vec{\mathbf{r}}\,'-\vec{\mathbf{r}})}{|\vec{\mathbf{r}}\,'-\vec{\mathbf{r}}|^3}\cdot\vec{\mathbf{J}}(\vec{\mathbf{r}}\,')\, d\vec{\mathbf{r}}\,', \qquad (2.2)$$

where $\vec{\mathbf{r}}$ is a point outside V_0 and $\vec{\mathbf{e}}(\vec{\mathbf{r}})$ is the unit normal vector w.r.t. the surface where the magnetometer is located. We remark that the knowledge of the normal component uniquely determines the magnetic field in the outer space [11].

Now, let $\vec{\mathbf{q}}_l$, $l = 1,\dots,N$, be the magnetometer locations and let $M = \{m_1,\dots,m_N\}$ be the corresponding measurements. In order to reconstruct the current distribution $\vec{\mathbf{J}}$ we would like to minimize the discrepancy $\Delta(\vec{\mathbf{J}}) := \left\| G(\vec{\mathbf{J}}) - M \right\|^2_{\mathbf{R}^N}$, with $G(\vec{\mathbf{J}}) = \{B_e(\vec{\mathbf{J}},\vec{\mathbf{q}}_1),...,B_e(\vec{\mathbf{J}},\vec{\mathbf{q}}_N)\}$. Unfortunately, there exist silent currents, so that non unique solutions can be expected. Moreover, the magnetic data can be affected by high noise. A regularization mechanism is required both to identify uniquely the solution by taking advantage of possible prior knowledge (in this case the spatial joint-sparsity of the currents) and to remove the noise.

III. The Magnetic Inverse Problem with Sparsity Constraints

We are interested in applications where the current density is spatially inhomogeneous so that it can be represented as a sum of weighted basic currents with only few significant terms. This means that we can assume $\vec{\mathbf{J}} = (J_1, J_2, J_3) \in L_2(V_0;\mathbf{R}^3)$ *sparsely* represented by a suitable dictionary $\mathcal{D} := (\psi_\lambda)_{\lambda\in\mathbf{\Lambda}}$, i.e.

$$J_\ell \approx \sum_{\lambda\in\mathbf{\Lambda}_S} j^\ell_\lambda\, \psi_\lambda\,, \qquad j^\ell_\lambda = \langle J_\ell, \psi_\lambda\rangle\,,\ \ell = 1,2,3, \qquad (3.3)$$

where $\Lambda_S \subset \Lambda$, the small set of significant coefficients, is the same for all the components. As a dictionary we can choose a stable multiscale basis, for instance a wavelet basis or frame [3], [4].

Thus, the magnetic inverse problem with the sparsity constraint $\mathbf{\Psi}_\mathcal{D}$ consists in minimizing the functional

$$\mathcal{J}_\mathbf{\Psi}(\vec{\mathbf{j}}, v) = \Delta(\vec{\mathbf{j}}) + \mathbf{\Psi}_\mathcal{D}(\vec{\mathbf{j}}, v), \qquad (3.4)$$

with respect to both $\vec{\mathbf{j}} = (j^\ell_\lambda)_{\lambda\in\mathbf{\Lambda},\ell=1,2,3}$ and an auxiliary weight v, restricted to $v_\lambda \geq 0$.

We use as sparsity constraint the *joint sparsity measure* introduced in [9], i.e.

$$\mathbf{\Psi}_\mathcal{D}(\vec{\mathbf{j}}, v) = \sum_{\lambda\in\mathbf{\Lambda}} v_\lambda\, \|\vec{\mathbf{j}}_\lambda\|_p + \sum_{\lambda\in\mathbf{\Lambda}} \omega_\lambda \|\vec{\mathbf{j}}_\lambda\|_2^2 + \sum_{\lambda\in\mathbf{\Lambda}} \theta_\lambda(\rho_\lambda - v_\lambda)^2, \qquad (3.5)$$

where $p \geq 1$ and $(\theta_\lambda)_{\lambda\in\mathbf{\Lambda}}$, $(\rho_\lambda)_{\lambda\in\mathbf{\Lambda}}$, $(\omega_\lambda)_{\lambda\in\mathbf{\Lambda}}$ are positive parameter sequences. Here, $\|\cdot\|_p$ denotes the usual p-norm for vectors in $\mathbf{R}^3$. In this way, the minimization of $\mathcal{J}_\mathbf{\Psi}$ promotes that all the entries of the vector $\vec{\mathbf{j}}_\lambda = (j^\ell_\lambda)_{\ell=1,2,3}$ have the *same sparsity* pattern.

By using the decomposition (3.3), the minimum problem reduces to minimization of the functional

$$\mathcal{J}_\mathbf{\Psi}(\vec{\mathbf{j}}, v) = \left\| T\vec{\mathbf{j}} - M \right\|^2_{\mathbf{R}^N} + \mathbf{\Psi}_\mathcal{D}(\vec{\mathbf{j}}, v), \qquad (3.6)$$

where the entries of $T\vec{\mathbf{j}}$ are given by

$$\begin{aligned}(T\vec{\mathbf{j}})_l \;=\; & \sum_{\ell=1}^{3}\sum_{\lambda\in\mathbf{\Lambda}} j^\ell_\lambda \frac{\mu_0}{4\pi} \\ & \int_{V_0} \left(\frac{\vec{\mathbf{e}}(\vec{\mathbf{q}}_l)\times(\vec{\mathbf{r}}\,'-\vec{\mathbf{q}}_l)}{|\vec{\mathbf{r}}\,'-\vec{\mathbf{q}}_l|^3}\right)_\ell \psi_\lambda(\vec{\mathbf{r}}\,')\, d\vec{\mathbf{r}}\,'.\end{aligned} \qquad (3.7)$$

An efficient iterative algorithm to numerically solve this minimum problem will be illustrated in the following Section.

IV. An accelerated iterative thresholding algorithm

The minimizer of the functional $\mathcal{J}_{\mathbf{\Psi}}$ can be approximated by an accelerated projected gradient method, deduced by combining the iterative thresholding algorithm given in [10], with the accelerated *projected gradient method* proposed in [5].

The iterative thresholding algorithm is as follows (cf. [2],[12]).

Algorithm JS

$$\begin{cases} \textit{Choose the sequences} \quad \theta, \rho, \omega \\ \textit{Pick an arbitrary} \quad \vec{\mathbf{j}}^{(0)} \in \ell_2(\Lambda; \mathbf{R}^3) \\ \textit{For} \quad 0 \le k \le K \quad \textit{do} \\ \qquad \vec{\mathbf{j}}^{(k+1)} = S^{(p)}_{\theta,\rho,\omega}\left(\vec{\mathbf{j}}^{(k)} + T^*M - T^*T\,\vec{\mathbf{j}}^{(k)}\right) \end{cases}$$

The operator $\mathcal{S}^{(p)}_{\theta,\rho,\omega}$ is a vector-valued thresholding operator whose explicit expression depending on the parameters can be found in [10].

Following the approach in [5] we define the set

$$\begin{aligned} C_{\theta,\rho,\omega}(R) \quad := \quad & \{\vec{\mathbf{j}} \in \ell_2(\mathbf{\Lambda}; \mathbf{R}^3) : \Psi_{\mathcal{D}}(\vec{\mathbf{j}}, v) \le R, \\ & \qquad \text{for some } 0 \le v \le \rho\}. \end{aligned}$$

The set $C_{\theta,\rho,\omega}(R)$ is convex whenever $\omega_\lambda \theta_\lambda \ge \frac{\kappa}{4}$ for all $\lambda \in \Lambda$, where $\kappa = 3$ for $p = 1$, and $\kappa = 1$ for $p \in \{2, \infty\}$, compare [9, Proposition 2.1]. See Figure IV for examples of these sets for different parameters, also in case of violation of the convexity.

The projected gradient iteration has the form:

Algorithm PG

$$\begin{cases} \textit{Pick an arbitrary} \quad \vec{\mathbf{j}}^{(0)} \in \ell_2(\Lambda; \mathbf{R}^3) \\ \textit{For} \quad 0 \le k \le K \quad \textit{do} \\ \qquad \textit{Choose the descent parameter} \quad \beta^{(k)} \\ \qquad \vec{\mathbf{j}}^{(k+1)} = \mathcal{P}_{C_{\theta,\rho,\omega}(R)}\big(\vec{\mathbf{j}}^{(k)} + \beta^{(k)}(T^*M - T^*T\,\vec{\mathbf{j}}^{(k)})\big) \end{cases}$$

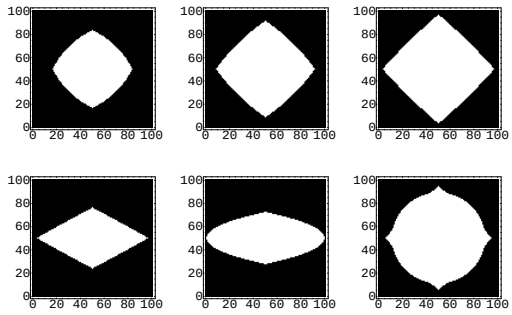

Fig. 1. The sets $C_{\theta,\rho,\omega}(R)$ in $\mathbf{R}^2$ (no vector components are considered and Λ contains two indexes only) for different parameters θ, ρ, ω, R.

where $\mathcal{P}_{C_{\theta,\rho,\omega}(R)}$ is the orthogonal projection onto $C_{\theta,\rho,\omega}(R)$.

This projection can be computed in practice by an adaptive thresholding choice: for any $\vec{\mathbf{j}} \in \ell_2(\Lambda; \mathbf{R}^3)$ there exists a $\eta := \eta(\vec{\mathbf{j}}, \theta, \rho, \omega, R) > 0$ such that

$$\mathcal{P}_{C_{\theta,\rho,\omega}(R)}(\vec{\mathbf{j}}) = \mathcal{S}^{(p)}_{\frac{\theta}{\eta},\eta\rho,\eta\omega}(\vec{\mathbf{j}}). \tag{4.8}$$

This relationship is promptly seen by using the definition of $\mathcal{S}^{(p)}_{\theta,\rho,\omega}$: choose $\eta > 0$ such that $\mathcal{S}^{(p)}_{\frac{\theta}{\eta},\eta\rho,\eta\omega}(\vec{\mathbf{j}}) \in \partial C_{\theta,\rho,\omega}(R)$, i.e., $\mathbf{\Psi}_{\mathcal{D}}(\mathcal{S}^{(p)}_{\frac{\theta}{\eta},\eta\rho,\eta\omega}(\vec{\mathbf{j}}), v) = R$ for some v and $\mathbf{\Psi}_{\mathcal{D}}(\mathcal{S}^{(p)}_{\frac{\theta}{\eta},\eta\rho,\eta\omega}(\vec{\mathbf{j}}), v') \ge R$ for all v'. Then

$$\begin{aligned} \mathcal{S}^{(p)}_{\frac{\theta}{\eta},\eta\rho,\eta\omega}(\vec{\mathbf{j}}) \quad &= \quad \arg\min_{\vec{\mathbf{j}}', v'} \|\vec{\mathbf{j}} - \vec{\mathbf{j}}'\|^2_{\mathbf{R}^3} + \eta \mathbf{\Psi}_{\mathcal{D}}(\vec{\mathbf{j}}', v) \\ &= \quad \arg\min_{\vec{\mathbf{j}}' \in C_{\theta,\rho,\omega}(R), v'} \|\vec{\mathbf{j}} - \vec{\mathbf{j}}'\|^2_{\mathbf{R}^3} + \eta \mathbf{\Psi}_{\mathcal{D}}(\vec{\mathbf{j}}', v) \\ &= \quad \arg\min_{\vec{\mathbf{j}}' \in C_{\theta,\rho,\omega}(R)} \|\vec{\mathbf{j}} - \vec{\mathbf{j}}'\|^2_{\mathbf{R}^3} + \eta R \\ &= \quad \mathcal{P}_{C_{\theta,\rho,\omega}(R)}(\vec{\mathbf{j}}). \end{aligned}$$

The fast convergence of Algorithm PG depends on a suitable choice of the *adaptive descent parameter*: following the arguments in [5] it is possible to show that the sequence $(\vec{\mathbf{j}}^{(k)})$ weakly converges to the minimizer of $\mathcal{J}_{\mathbf{\Psi}}$ which lies on the set $C_{\theta,\rho,\omega}(R)$ if the sequence $\beta^{(k)}$ satisfies the conditions

$$\begin{cases} \bar{\beta} := \sup\{\beta^{(k)}, k \in \mathbf{N}\} < \infty\,, \\ \inf\{\beta^{(k)}, k \in \mathbf{N}\} \ge 1\,, \\ \beta^{(k)} \|T(\vec{\mathbf{j}}^{(k+1)} - \vec{\mathbf{j}}^{(k)})\|^2 \le r \|\vec{\mathbf{j}}^{(k+1)} - \vec{\mathbf{j}}^{(k)}\|^2\,, \ k \ge k_0\,, \end{cases} \tag{4.9}$$

where $r := \|T^*T\|_{\ell_2 \to \ell_2} < 1$ and k_0 is a suitable index.

Since at each iteration the evaluation of the action of T^*T is requested, we wonder whether such evaluation can be compressed and performed in a fast way.

Let $\mathcal{M}$ be the matrix whose entries are the coordinates of T^*T in the multiscale basis $(\psi_\lambda)_{\lambda\in\Lambda}$, i.e.

$$\left(T^*T\vec{\mathbf{j}}\right)_{\lambda,\ell} = \sum_{\mu\in\mathbf{\Lambda}}\sum_{m=1}^{3} j_\mu^m\, \mathcal{M}_{(\lambda,\ell),(\mu,m)}, \tag{4.10}$$

for $\lambda\in\Lambda, \ell = 1,2,3$. From (3.7) it follows

$$\mathcal{M}_{(\lambda,\ell),(\mu,m)} := \sum_{l=1}^{N} (A_{\ell,l}\psi_\lambda)(A_{m,l}\psi_\mu), \tag{4.11}$$

$$\lambda,\mu\in\Lambda, \ell, m = 1,2,3,$$

where

$$A_{i,l}\,\psi_\lambda = \frac{\mu_0}{4\pi}\int_{V_0}\left(\frac{\vec{\mathbf{e}}(\vec{\mathbf{q}}_l)\times(\vec{\mathbf{r}}\,'-\vec{\mathbf{q}}_l)}{|\vec{\mathbf{r}}\,'-\vec{\mathbf{q}}_l|^3}\right)_\ell \psi_\lambda(\vec{\mathbf{r}}\,')\,d\vec{\mathbf{r}}\,'. \tag{4.12}$$

It can be shown that $\mathcal{M}$ has compressibility properties w.r.t. a compactly supported wavelet basis (see [8]) so that $T^*T\,\vec{\mathbf{j}}^{(k)}$ can be efficiently evaluated.

V. A BIDIMENSIONAL TEST

In the numerical tests the magnetic data are generated by three horizontal bidimensional current dipoles located in the plane $\Pi_0 = \{x, y\in\mathbf{R}, z = 0\}$. The magnetic field is sampled by 400 magnetometers located on a regular horizontal grid at height $\delta = 1$. Note that we use adimensional measure units in the tests.

This setting can be used to model both the problem of localizing shallow neural sources and non destructive testing of thin structures. In fact, the current dipoles can be viewed both as sources of brain activity and as discontinuities in a given current distribution. We remark that in the bidimensional case the inverse problem has a unique solution, nevertheless, it can be ill-conditioned for the presence of noise.

As a multiscale basis, we choose the Daubechies orthonormal wavelets with $d = 4$ vanishing moments and discretize the plane Π_0 with 32 pixels for each dimension. Finally, 2 multiscale levels are used for the current decomposition.

We performed some preliminary tests on Algorithm JS with the thresholding parameter tuned following [9], [10]. In particular, for all $\lambda\in\Lambda$ we choose $\rho_\lambda = 10^{-4}$ in the noiseless case, and $\rho_\lambda = 4\cdot 10^{-3}$ in the noisy case. As for the other parameters, we fix $\theta_\lambda = 10^{-4}$ and $\omega_\lambda = 0$ for all $\lambda\in\Lambda$, thus in the sequel we will suppress the indexes θ,ω from the thresholding operator, that will be simply addressed as $\mathcal{S}_\rho^{(p)}$. In Fig. 3 the reconstructed current distribution after 100 iterations by soft-thresholding, i.e. Algorithm JS with $p = 1$, is shown. In Fig. 5 the current distribution reconstructed is displayed when high white Gaussian noise with linear signal to noise ratio equal to 0.1 is added to the magnetic field (see Fig. 4). In spite of the high level of noise and of the poor discretization of the plane, 32 linear pixels, it is still possible to localize the current sources.

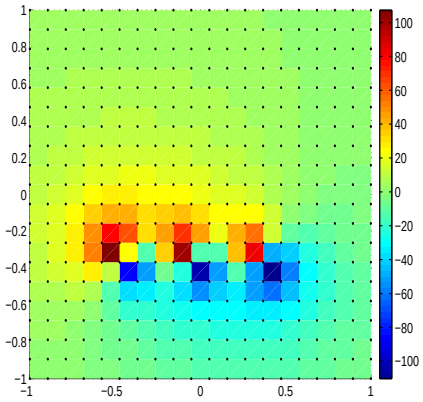

Fig. 2. The magnetic field produced by three current dipoles located in $(-0.5,-0.4,0)$, $(-0.1,-0.4,0)$, $(0.3,-0.4,0)$. The black points represent the magnetometer sites.

As a comparison, in Fig. 6 we show localization results obtained by means of quadratic Tikhonov regularization in the case when the data are distorted by high noise. In real fact, quadratic Tikhonov regularization is not able to give a satisfactory localization of the current sources: when the regularization parameter is low (equal to 10^{-3} in the example) the current is not reconstructed at all (Fig. 6, left), while a greater regularization parameter blurres the image (Fig. 6, right, where the regularization parameter is chosen by means of the discrepancy principle and is equal to 356).

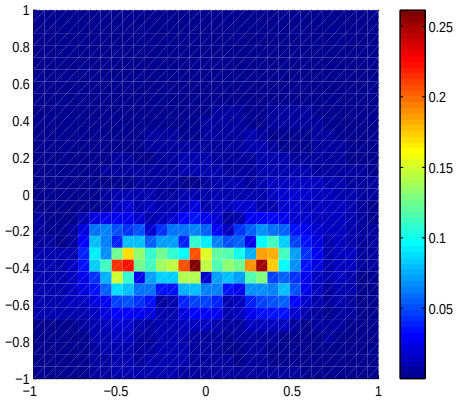

Fig. 3. The current intensity reconstructed starting from the magnetic field displayed in Fig. 2 by using soft-thresholding with $\tau = 10^{-4}$.

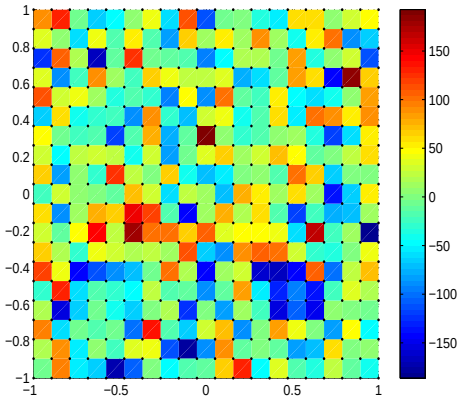

Fig. 4. The noisy magnetic field produced by three current dipoles located in $(-0.5, -0.4, 0)$, $(-0.1, -0.4, 0)$, $(0.3, -0.4, 0)$. The magnetometer distribution is represented by black points.

VI. Conclusions

The numerical tests presented in the previous Section show that Algorithm JS behaves better than classical quadratic Tikhonov regularization in case of high noise, and represent promising results for the reconstruction of current sources, in spite of the poor discretization with just 32 linear pixels. We proposed further Algorithm PG as an acceleration of Algorithm JS generalizing the approach introduced in [5] to the case of a joint-sparsity constraint.

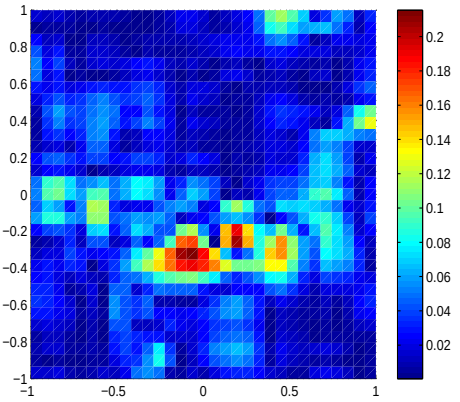

Fig. 5. The current intensity reconstructed starting from the magnetic field displayed in Fig. 4 by using soft-thresholding with $\tau = 4 \cdot 10^{-3}$.

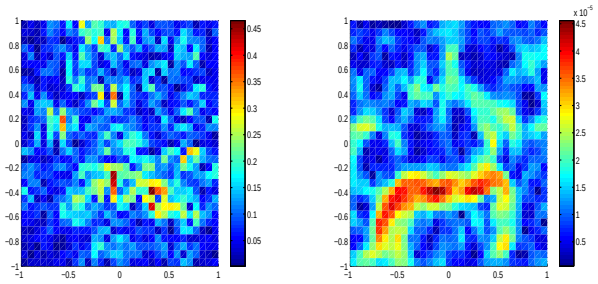

Fig. 6. The current distribution reconstructed by using the quadratic Tikhonov regularization starting from the noisy magnetic field displayed in Fig. 4. Two different values of the regularization parameter have been used: 0 (right) and 356 (right).

References

[1] J.R. Bradley, J.P. Wikswo, N.G. Sepulveda, Using a magnetometer to image a two-dimensional current distribution, *J. App. phys.* 65 (1989), pp. 361–372.

[2] G. Bretti, F. Pitolli, An iterative thresholding algorithm for the neural current imaging, preprint.

[3] O. Christensen, An introduction to frames and Riesz bases, Birkhäuser, Boston, 2003.

[4] I. Daubechies, Ten Lectures on Wavelets, *SIAM*, 1992.

[5] I. Daubechies, M. Fornasier, I. Loris, Accelerated projected gradient methods for linear inverse problems with sparsity constraints, *J. Fourier Anal. Appl.*, **14** (2008), pp. 764-792.

[6] I. Daubechies, M. Defrise, C. De Mol, An iterative thresholding algorithm for linear inverse problems with a sparsity constraint, *Comm. Pure Appl. Math.* , **57** (2004), pp. 1413-1457.

[7] H.W. Engl, M. Hanke, A. Neubauer, Regularization of inverse problems, Kluwer Academic Publishers, Dordrecht, 1996.

[8] M. Fornasier, F. Pitolli, Adaptive iterative thresholding algorithms for magnetoencephalography, *J. Comput. Appl. Math.*, **221** (2008), pp. 386-395.

[9] M. Fornasier, H. Rauhut, Recovery algorithms for vector valued data with joint sparsity constraints, *SIAM J. Numer. Anal.*, **46** (2008), pp. 577-613.

[10] M. Fornasier, H. Rauhut, Iterative thresholding algorithms, *Appl. Comput. Harmon. Anal.*, **25** (2008), pp. 187-208.

[11] R. Kress, L. Kühn, R. Potthast, Reconstruction of a current distribution from its magnetic field, *Inverse Problem*, **18** (2002), pp. 1127–1146.

[12] F. Pitolli, G. Bretti, An iterative algorithm with joint sparsity constraints for magnetic tomography, preprint.

[13] J. Sarvas, Basic mathematical and electromagnetic concepts of the biomagnetic inverse problem, *Phys. Med. Biol.*, **32** (1987), pp. 11–22.

[14] J.P. Wikswo, Applications of SQUID magnetometers to biomagnetism and nondestructive evaluation, in *Applications of Superconductivity* (H. Weinstock ed.), Kluwer Academic Publishers, Dordrecht, 2000, pp. 139–228.